COMPUTATIONAL ANALYSIS ON HEAVE AND PITCH MOTIONS PERFORMANCE OF A HYDROFOIL SHIP

A. Fitriadhy[1], N. Amira Adam[2], and M. Syafiq Zikry[3]

[1] Faculty of Ocean Engineering Technology and Informatics, Universiti Malaysia Terengganu, Kuala Terengganu, Terengganu, Malaysia
[2] Postgraduate Student, Faculty of Ocean Engineering Technology and Informatics, Universiti Malaysia Terengganu, Kuala Terengganu, Terengganu, Malaysia
[3] Undergraduate Student, Faculty of Ocean Engineering Technology and Informatics, Universiti Malaysia Terengganu, Kuala Terengganu, Terengganu, Malaysia

E-mail: naoe.afit@gmail.com

ABSTRACT

Hydrofoil ship usually experiences high resistance and excessive heave and pitch that may lead to downgrade her seakeeping performance. Therefore, a reliable investigation on prediction of a seakeeping performance of a hydrofoil ship in head-seas is obviously required. To achieve this objective, an analysis of Computational Fluid Dynamic (CFD) approach on hydrofoil ship motion is then proposed. Several parameters such as angle of stern foil and Froude Number have been accordingly taken into account in the simulation, where the fore foil angle is constantly 5°. In general, the results revealed that the increase of the stern foil angle was proportional to the heave motion of the hydrofoil ship. As compared to the magnitude of the stern foil angle of 5° and 10°, the heave motion of the hydrofoil ship has sufficiently decreased at the stern foil angle of 7.5°, which leads to have a better seakeeping performance. Furthermore, the subsequent increase of Froude number pointing towards reduction of heave motion, which was inversely proportional to the magnitude of her pitch motion. Inherently, these have led to degrade of the hydrofoil ship seakeeping performances presented in the form of high Response Amplitude Operators (RAO). In general, this CFD simulation is very beneficial to ensure an operational effectiveness of hydrofoil design in high sea states with respect to the aforementioned design parameter.

Keyword: CFD, hydrofoil, angle of stern foil, heave, pitch

Introduction

Basically, hydrofoil ship usually consists of a wing like structure mounted on struts below the hull called as foil. This foil provides vertical force to rise up the ship out of the water surface during sailing. Therefore, this foil structure plays an important role in the design of the hydrofoil ship to minimize the drag force as well as reducing the ship's draft and her wetted surface area. As a result, the hydrofoil ship has dealt with less fuel consumption and increased marine eligibility, Matveev and Duncan (2005).

As a common ship, a seakeeping performance of the hydrofoil ship is a very prominent aspect to be analyzed in the early design stage. Several researchers had studied on the ship seakeeping behavior via numerical and experimental approaches. Faltinsen (1971) and Ma et al. (2016) investigated on seakeeping analysis by using the theoretical method. This approach is very efficient and requires relatively small computer resources. However, this method requires a very large data base of ship characteristics. The problem of organizing such a data base becomes the main difficulty of applying the method. In addition, (Islam, Jahra, & Hiscock, 2016; Sun, Yao, Xiong, & Ye, 2017; Vakilabadi, Khedmati, & Seif, 2014; Yao, Sun, Wang, & Ye, 2017) have experimentally conducted model test at towing tank. Even so, the experimental method is a time-consuming, complex procedure process and costly; and even impractical for various seakeeping test configurations (Fitriadhy & Adam, 2017). Meanwhile, the accuracy of the typical

numerical approach requires necessarily further verification since some simplified simulation conditions were assumed to be given. Whilst a Computational Fluid Dynamic (CFD) approach for assessing the seakeeping performance on the hydrofoil ship put very demanding requirements with regards to a more reliable result both of accuracy and precision. According to Vakilabadi et al. (2014), the seakeeping results of the tests are used to produce transfer functions for heave and pitch motions, where the non-dimensional are called Response Amplitude Operators (RAOs). The study from Fitriadhy, Razali, and Aqilah Mansor (2017) and Fitriadhy and Adam (2017) found that the seakeeping quality of the ship has been improved by presented the sufficient reduction of the RAO. In addition, the fully submerged hydrofoil control system was applied to control her vertical motion, Kim and Yamato (2004) and Kim and Yamato (2005). Similarly, Bai and Kim (2010) employed various types of control algorithms, and found that PID controller reduced effectively the vertical motion of the hydrofoil ship in the absence of incident waves.

This paper presents Computational Fluid Dynamic (CFD) analysis on heave and pitch motions of a hydrofoil ship. Several parameters such as various angles of stern foil and Froude numbers have been taken into account. Commercial CFD software, namely Flow3D, was utilized by applying the incompressible unsteady Reynolds-Averaged Navier Stokes equations in which RANSE and continuity equations are discretized by the finite volume method based on Volume of Fluid (VOF) to deal with the non- linear free surface. In addition, the mesh generation, boundary condition, initial condition and numerical option were carefully determined before simulations. Basically, this simulation solved the mesh independent study to select the optimal domain discretization. The Response Amplitude Operator (RAO) of heave and pitch motion performances are then discussed.

Mathematical Equation

Basically, two equations in accordance with the law conservation of mass and momentum as clearly expressed in Eqs. (1)-(4). The current CFD simulation is based on the incompressible unsteady RANSE, which employs the volume of fluid (VOF).

Continuity and Momentum Equations

The general mass continuity equation is presented in Eq. (1), for a moving object and the comparative VOF function transport equation; where the VF is the fractional volume open to flow, ρ is the fluid density, $RDIF$ is a turbulent diffusion term, $RSOR$ is a mass source and Ax, Ay and Az is the fractional area open to flow in x, y and z-direction, respectively (Manual, 2011).

$$V_F \frac{\partial \rho}{\partial t} + \frac{\partial}{\partial x}(\rho u A_x) + R\frac{\partial}{\partial y}(\rho v A_y) + \frac{\partial}{\partial z}(\rho \omega A_z) + \xi \frac{\rho u A_x}{x} = R_{DIF} + R_{SOR} \tag{1}$$

The momentum theory also applies in three coordinates direction (u, v, w) that has been used in the motion equation as displayed in Eqs. (2)-(4).

$$\frac{\partial u}{\partial t} + \frac{1}{V_F}\left\{uA_x\frac{\partial u}{\partial x} + vA_yR\frac{\partial u}{\partial y} + uA_z\frac{\partial u}{\partial z}\right\} - \xi\frac{A_y v^2}{xV_F} \tag{2}$$
$$= -\frac{1}{\rho}\frac{\partial p}{\partial x} + G_x + f_x - b_x - \frac{R_{SOR}}{\rho V_F}(u - u_w - \delta u_s)$$

$$\frac{\partial v}{\partial t} + \frac{1}{V_F}\left\{uA_x\frac{\partial v}{\partial x} + vA_yR\frac{\partial v}{\partial y} + uA_z\frac{\partial v}{\partial z}\right\} + \xi\frac{A_y uv}{xV_F} \tag{3}$$
$$= -\frac{1}{\rho}(R)\frac{\partial p}{\partial y} + G_y + f_y - b_y - \frac{R_{SOR}}{\rho V_F}(v - v_w - \delta v_s)$$

$$\frac{\partial w}{\partial t} + \frac{1}{V_F}\left\{uA_x\frac{\partial w}{\partial x} + vA_yR\frac{\partial w}{\partial y} + uA_z\frac{\partial w}{\partial z}\right\} = -\frac{1}{\rho}\frac{\partial p}{\partial z} + G_z + f_z - b_z - \frac{R_{SOR}}{\rho V_F}(w - w_w - \delta w_s) \tag{4}$$

where (Gx, Gy, Gz) are body accelerations, (fx, fy, fz) are viscous accelerations and (bx, by, bz) are flow losses in porous media or across porous baffle plates, and the final condition account for the injection of mass at a source represented by a geometry element (Manual, 2011).

Turbulence Model

In the current CFD simulation, Renormalization-group (RNG) turbulence model has been selected considering for low Reynolds number effects (Koutsourakis, Bartzis, & Markatos, 2012; A. Yakhot, Rakib, & Flannery, 1994; V. Yakhot & Orszag, 1986). Through applying the double averaging strategy to the transport equations for Turbulent Kinetic Energy (TKE) and its dissipation rate produces the turbulence model for the flow as displayed in Eqs. (5)-(8).

$$\frac{\delta k}{\delta t} + U_j\frac{\delta k}{\delta x_j} = \frac{\delta}{\delta x_j}\left[\left(v + \frac{v_t}{\sigma_k}\right)\frac{\delta k}{\delta x_j}\right] + P_k + B_k + W_k \tag{5}$$

$$\frac{\delta\varepsilon}{\delta t} + U_j\frac{\delta\varepsilon}{\delta x_j} = \frac{\delta}{\delta x_j}\left[\left(v + \frac{v_t}{\sigma_\varepsilon}\right)\frac{\delta\varepsilon}{\delta x_j}\right] + C_{1\varepsilon}\frac{\varepsilon}{k}(P_k + B_k)(1 + C_{3\varepsilon}R_f) + W_\varepsilon - C_{2\varepsilon}^*\frac{\varepsilon^2}{k} \tag{6}$$

$$P_k = v_t S^2 = v_t\left(\frac{\delta U_i}{\delta x_j} + \frac{\delta U_j}{\delta x_i}\right)\frac{\delta U_i}{\delta x_j} \tag{7}$$

$$B_k = \beta g_i\frac{v_t}{\sigma_s}\frac{\delta s}{\delta x_i} \tag{8}$$

where P_k is the shear production term of TKE, $S = 2\overline{S_{ij} S_{ji}}$ is the average of strain tensor and $S_{ij} = \frac{1}{2}\frac{\delta U_i}{\delta x_j} + \frac{\delta U_j}{\delta x_i}$, B_k and W_k is the is the buoyant and wake production term of TKE, respectively. In addition, W_ε is the wake production term in ε, σk and $\sigma \varepsilon$ are the turbulent Prandtl numbers for k and ε, and $C_{i\varepsilon}$, $C3\varepsilon$ and $C*_{2\varepsilon}$ are model coefficients.

Heave and Pitch Motions

In these equations, M is the vessel mass, I5 is the moment of inertia in pitch and A_ih, B_ij, and C_ij are coefficient of added mass, damping and restoring coefficient, respectively. Also, F3 and F5 are vertical force and longitudinal subverting moment on the vessel respectively (Seif, Mehdigholi & Najafi, 2014).

The degree of freedom (D.O.F) represented the possible translations and rotation of the body. The heave and pitch motion noted as translation and rotation respectively along X, Y and Z axis that define the behaviour of the hydrofoil ship during sailing. Heave motion is the linear vertical upward and downward acceleration of ships along their vertical axis.

Besides, the pitch motion occurred at ship's motion lifted at the bow and lowered at stern and vice versa. The equations are demonstrated as Eqs. 9 and 10.

$$(M + A_{33})\frac{d^2\eta_3}{dt_2} + B_{33}\frac{d\eta_3}{dt} + C_{33}\eta_3 + A_{35}\frac{d^2\eta_5}{dt_2} + B_{35}\frac{d\eta_5}{dt} + C_{35}\eta_5 = F_3 \quad (9)$$

$$A_{53}\frac{d^2\eta_3}{dt_2} + B_{53}\frac{d\eta_3}{dt} + C_{53}\eta_3 + (I_{55} + A_{35})\frac{d^2\eta_5}{dt_2} + B_{35}\frac{d\eta_5}{dt} + C_{55}\eta = F_5 \quad (10)$$

Table 1. Dimensions of hydrofoil ship in full scale and model scale

Geometrical parameters	Full scale	Model scale
Length Overall, LOA (m)	32.64	16.32
Length Between Perpendicular, LBP (m)	32.276	16.138
Beam, B (m)	8.278	4.139
Draft, T (m)	1.4	0.7

Simulation Condition

Principle Data of Propeller

The 3D geometry of the hydrofoil ship is clearly shown in Figure 1. The details of the ship are completely summarized in Table 1.

Parametric Studies

In the current CFD simulation, several parametric studies such as various angles of stern foil and Froude numbers have been taken into consideration. Here, the bow foil angle magnitude of 5 with constant regular wave condition has been employed. The detailed parameter is completely summarized in Table 2.

Computational Domain and Mesh Generation

The computational domain is presented as structured mesh that is defined in a Cartesian. Each of the boundary conditions as shown in the mesh block 1 and mesh block 2, is displayed in Figure 2 (left). Referring to mesh block 1, the boundary condition at X_{min} is defined as wave, while X_{max} is defined by outflow boundary to absorb the wave motion which will reduce the reflection from the boundary. Y_{min}, Y_{max} and Z_{min} are assigned as symmetry boundary which it applies zero-gradient condition at the boundary and Z_{max} using specified pressure to create a uniform pressure in the boundary. All mesh boundaries for mesh block 2 are defined by symmetry. The boundary conditions for the current CFD simulations are completely presented in Table 3.
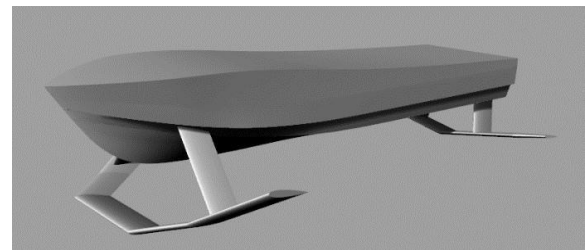

Figure 1. 3D model of a hydrofoil ship

Table 2. Matrix of computational simulation

Froude No.	Angle of stern foil (degree)		
	5	7.5	10
1.382	-	√	-
1.423	-	√	-
1.545	-	√	-
1.626	√	√	√
1.708	-	√	-
1.830	-	√	-

Table 3. Boundary conditions

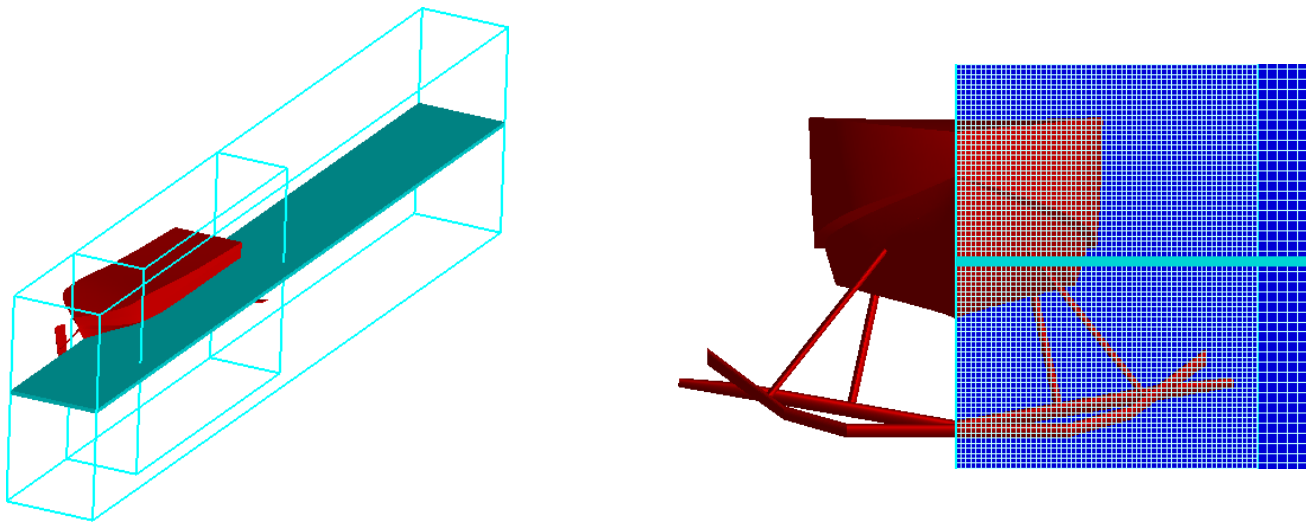| Boundary	Mesh block 1	Mesh block 2
Xmin	Wave	Symmetry
Xmax	Outflow	Symmetry
Ymin	Symmetry	Symmetry
Ymax	Symmetry	Symmetry
Zmin	Symmetry	Symmetry
Zmax	Specified Pressure	Symmetry

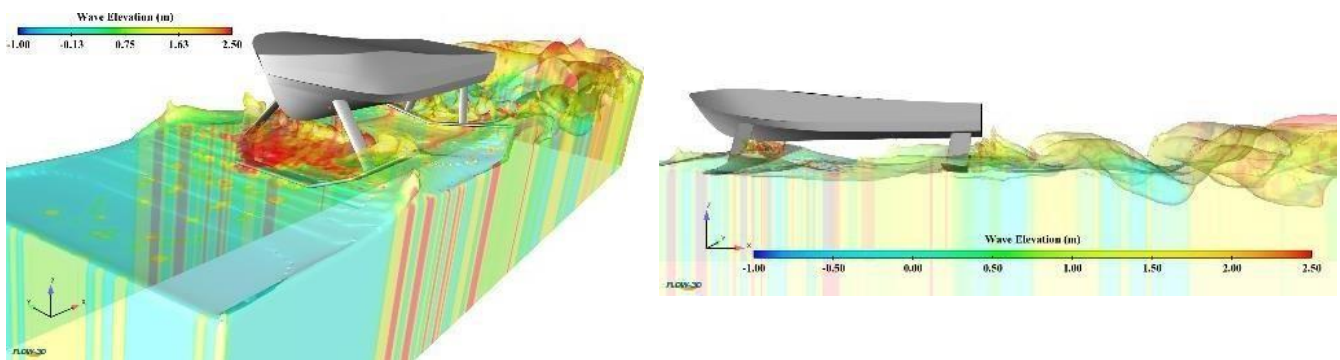**Figure 2.** Overall mesh block using in simulation

Figure 3. Example visualization of hydrofoil motion in waves

Referring to Table 4, four difference total number of cell meshing has been conducted to select an adequate number of cells meshing indicated by steadiness and computation time. In this research, the total number of cells meshing of 2,929,615 (case C) has been chosen to apply for all simulation. The increases of total number of cells meshing up to 3,536,935 (case D) was obviously unnecessary due to insignificant of percentage of difference.

Results and Discussion

The CFD simulations have been carried out to predict the heave and pitch motions performance of hydrofoil at the various angles of stern foil and Froude numbers. The simulation results have been displayed and discussed below.

Effect of Foil's Angle at the Stern

Referring to Fig. 4, the subsequent increase of angle of stern foil from 5° to 10° results in more significant influence to the heave and pitch motions of hydrofoils ship. It was noted that the heave motion remarkably increased up to 236.5% as the angle of stern foil increased from at 7.5° to 10°; meanwhile, her pitch motion was relatively steady. In addition, the pitch motion sufficiently decreased by 20.1% due to reduction of the stern foil angle of 5 to 7.5°. The results are completely presented in Table 4. Based on the current results, it is merely concluded that the vertical motions behaviour at the stern foil angle of 7.5° coupled with bow foil angle of 5° provides a better seakeeping performance indicated with the less magnitude of heave and pitch motions (see Figure. 5) compared to the stern foil angle of 5° and 10°. However, the large magnitude of heave and pitch motions at the stern foil angles of 5° and 10° have potentially degraded the seakeeping performance of the hydrofoil ship due to precence of the unfavorable vertical ship motions. This non-linearity in the hydrofoil motions introduced by the waves coupled with the hydrodynamic effect of the stern foil, which demands a more comprehensive investigation in dealing with this complex problem. This is similar to what was reported by Keuning (1979) and Reguram, Surendran, and Lee (2016), where the angle of foil produced the significant influence of ship's responses.
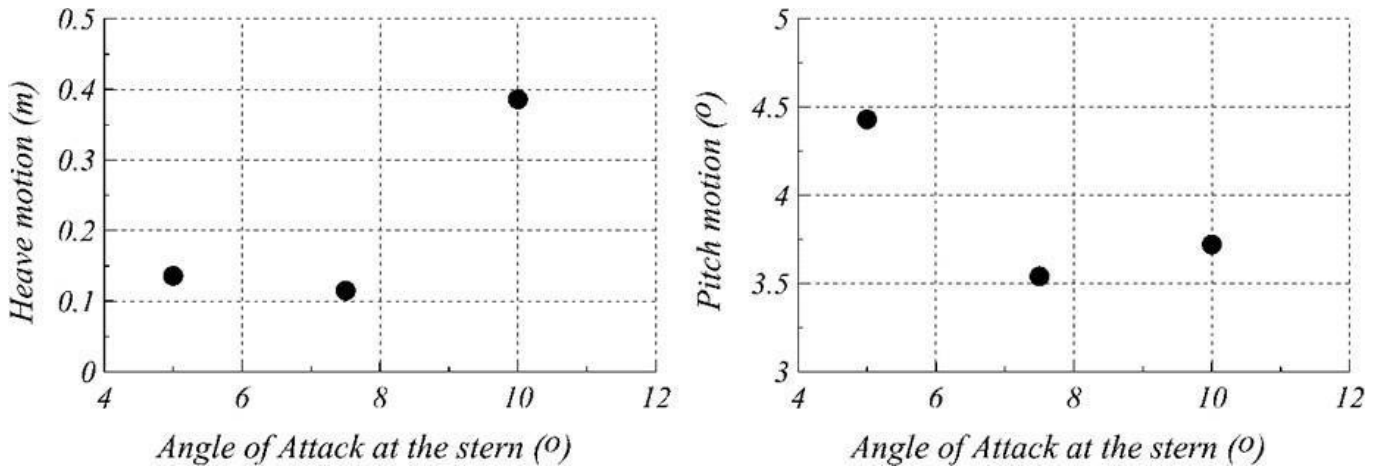
Figure 4. Heave (left) and pitch (right) motions characteristics at various angles of stern's foil, where the fore foil angle is 5°

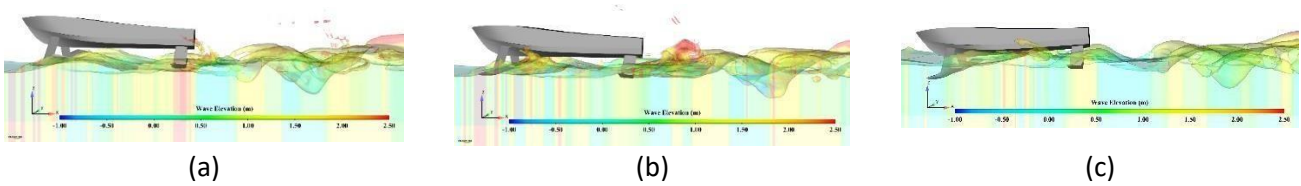(a)　　　　　　　　　　　(b)　　　　　　　　　　　(c)

Figure 5. Vertical motion of hydrofoil characteristics at various angle of stern foils (a) 5°, (b) 7.5° and (c) 10°, where the fore foil angle is 5° and Fr = 1.626
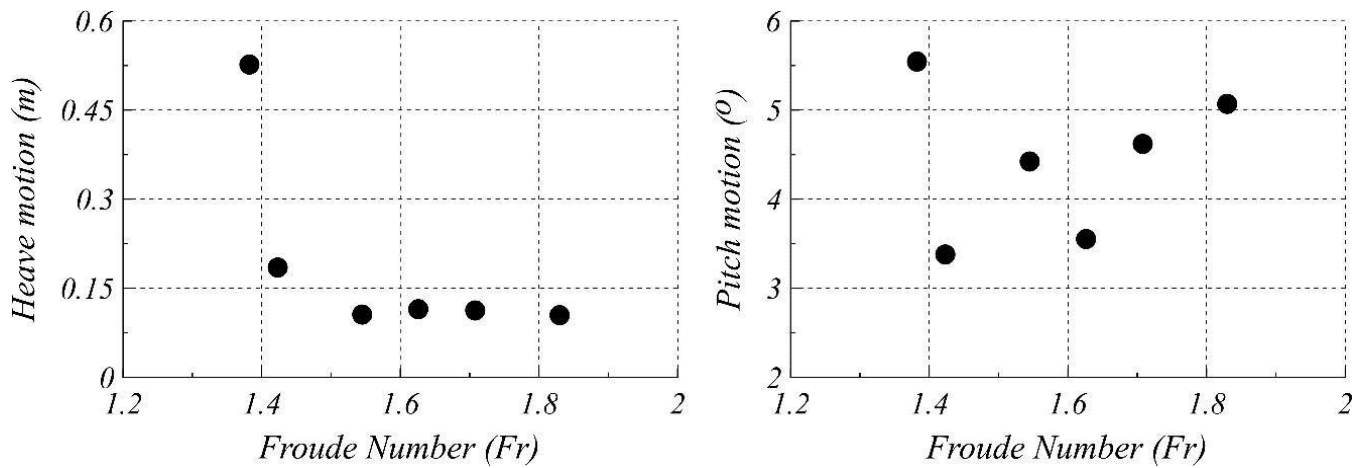

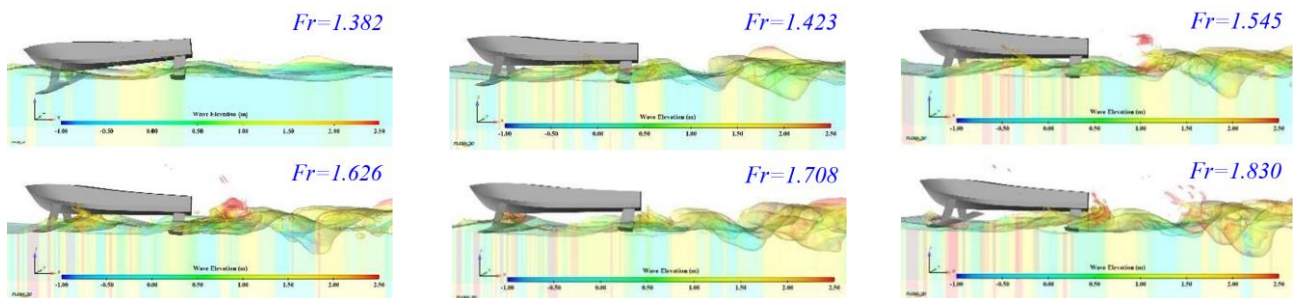**Figure 6.** Heave (left) and pitch (right) motions of various Froude numbers

Figure 7. Vertical motion of hydrofoil characteristics at various Froude numbers with angle of fore and stern foils are 5° and 7.5°, respectively

Table 5. Heave and pitch motions characteristics at various angle of stern foil

Angle of stern foil (◦)	Heave motion (m)	Pitch motion (◦)
5	0.1357	4.43
7.5	0.1147	3.54
10	0.3860	3.72

Effect of Various Froude Number (Fr) on Hydrofoil Ship

The heave and pitch motions of hydrofoil ship at various Froude numbers are displayed in Figure 6, where the results are completely summarized in Table 6.

Table 6. Heave and pitch motions for various Froude numbers

Froude number	Heave motion (m)	Pitch motion (◦)
1.382	0.5268	5.5463
1.423	0.1851	3.3816
1.545	0.1060	4.4231
1.626	0.1147	3.5523
1.708	0.1129	4.6204
1.830	0.1048	5.0699

The hydrofoil ship at Fr = 1.382 showed a significant influence where it resulted in the higher heave motion as compared with the case of the other forward velocities. It was pointed out here that the further increase of the Froude number (Fr > 1.545), the hydrofoil ship has constituted a steady-state condition for her heave motion characteristics. The finding was reasonable since the hydrofoil ship configurations requires appropriate speed to generate lifting forces and reduce the drag force between the wetted surface area and water surfaces (McCauley, 2018). In this condition, the hydrodynamics support allows the hydrofoil to remain an even keel condition and stable sailing with high positive dynamics pressure. This can be explained by the fact that the subsequent increase of Froude numbers led to decrease the drag, by lifting the hull out of water (see Figure 7). Looking into a nonlinear trend of her seakeeping behaviour in waves, the highest amplitude motion Adaofher heave and pitch motions at Fr = 1.382 were 0.5268 m and 5.5o, respectively. This indicated that the seakeeping behaviour of the hydrofoil ship gradually degraded, which can be explained by the fact that the hydrofoil ship had more vigorous heave and pitch motions, which was uncomfortable for the sailing (Keuning & Van Walree, 2006).

Conclusion

The simulation on predicting heave and pitch motions of the hydrofoil ship has successfully performed using the Computational Fluid Dynamics (CFD). The effect of the various angle of stern foil and Froude numbers in regular wave condition. The results are as follow:

- Through employing the stern foil angle of 7.5 coupled with bow foil angle of 5, the heave and pitch motions of the hydrofoil ship have sufficiently decreased, which may lead to provide a better seakeeping performance.
- The angle of stern foil has more significant effect to the seakeeping performances as compared to the effect of the forward velocities.

References

[1] J. Bai, & Y. Kim, Control of the vertical motion of a hydrofoil vessel, *Ships and Offshore Structures*. **5(3)** (2010) 189-198.

[2] O. Faltinsen, A rational strip theory of ship motions: Part II, 1971.

[3] A. Fitriadhy, & N.A. Adam, Heave and pitch motions performance of a monotricat ship in head-seas, *International Journal of Automotive and Mechanical Engineering*, **14** (2017) 4243-4258.

[4] A. Fitriadhy, N. Razali, & N. Aqilah Mansor, Seakeeping performance of a rounded hull catamaran in waves using CFD approach, *Journal of Mechanical Engineering and Sciences*. **11(2)** (2017) 2601-2614.

[5] M. Islam, F. Jahra, & S. Hiscock, Data analysis methodologies for hydrodynamic experiments in waves, *Journal of Naval Architecture and Marine Engineering*. **13(1)** (2016) 1-15.

[6] J. Keuning, A calculation method for the heave and pitch motions of a hydrofoil boat in waves, *International Shipbuilding Progress*. **26(302)** (1979).

[7] J. Keuning, & F. Van Walree, The comparison of the hydrodynamic behaviour of three fast patrol boats with special hull geometries, *Paper presented at the Proceedings of the 5th International Conference on High Performance Marine Vehicles*, 2006.

[8] S.-H. Kim, & H. Yamato, An experimental study of the longitudinal motion control of a fully submerged hydrofoil model in following seas, *Ocean Engineering*. **31(5-6)** (2004) 523-537.

[9] S. -H. Kim, & H. Yamato. The estimation of wave elevation and wave disturbance caused by the wave orbital motion of a fully submerged hydrofoil craft, *Journal of Marine Science and Technology*. **10(1)** (2005) 22-31.

[10] N. Koutsourakis, J.G. Bartzis, & N.C. Markatos. Evaluation of Reynolds stress, k-ε and RNG k-ε turbulence models in street canyon flows using various experimental datasets, *Environmental Fluid Mechanics*. (2012) 1-25.

[11] S. Ma, R. Wang, J. Zhang, W. Duan, R.C. Ertekin & X. Chen, Consistent formulation of ship motions in time-domain simulations by use of the results of the strip theory, *Ship Technology Research*. **63(3)** (2016) 146-158.

[12] Manual, F. D. U, Flow3D User Manual, v9. 4.2, Flow Science. Inc., Santa Fe, NM, 2011.

[13] K. Matveev, & R. Duncan, Development of the tool for predicting hydrofoil system performance and simulating motion of hydrofoil-assisted boats, Paper presented at the High Speed and High-Performance Ship and Craft Symposium, Everett/WA: ASNE, USA, 2005.

[14] J.L. McCauley, Hydrodynamic Lift on Boats. arXiv preprint arXiv:1808.03313, 2018.

[15] B.R. Reguram, S. Surendran, & S.K. Lee, Application of fin system to reduce pitch motion, *International Journal of Naval Architecture and Ocean Engineering*. **8(4)** (2016) 409-421.

[16] M. Seif, H. Mehdigholi, & A. Najafi, Experimental and numerical modeling of the high speed planing vessel motion, *Journal of Marine Engineering & Technology*. **13(2)** (2014) 62-72.

[17] X. Sun, C. Yao, Y. Xiong, & Q. Ye, Numerical and experimental study on seakeeping performance of a swath vehicle in head waves, *Applied Ocean Research*. **68** (2017) 262-275.

[18] K.A. Vakilabadi, M.R. Khedmati, & M.S. Seif, Experimental study on heave and pitch motion characteristics of a wave-piercing trimaran, *Transactions of FAMENA.* **38(3)** (2014) 13-26.

[19] A. Yakhot, S. Rakib, & W. Flannery, Low- Reynolds number approximation for turbulent eddy viscosity, *Journal of Scientific Computing.* 9(3) (1994) 283-292.

[20] V. Yakhot, & S.A. Orszag, Renormalization group analysis of turbulence I, Basic theory, *Journal of Scientific Computing*. 1(1) (1986) 3-51.

[21] C.-B. Yao, X.S. Sun, W. Wang, & Q. Ye, Numerical and experimental study on seakeeping performance of ship in finite water depth, *Applied Ocean Research*. 67 (2017) 59-77.